

Article

Numerical Simulation of Gas Phase Reaction for Epitaxial Chemical Vapor Deposition of Silicon Carbide by Methyltrichlorosilane in Horizontal Hot-Wall Reactor

Botao Song, Bing Gao ^{*}, Pengfei Han, Yue Yu  and Xia Tang 

The Institute of Technological Sciences, Wuhan University, Wuhan 430072, China; 2020106520027@whu.edu.cn (B.S.); 2020106520028@whu.edu.cn (P.H.); 2019106520025@whu.edu.cn (Y.Y.); 2018106520022@whu.edu.cn (X.T.)

* Correspondence: gaobing@whu.edu.cn

Abstract: Methyltrichlorosilane (CH_3SiCl_3 , MTS) has good performance in stoichiometric silicon carbide (SiC) deposition and can be facilitated at relatively lower temperature. Simulations of the chemical vapor deposition in the two-dimensional horizontal hot-wall reactor for epitaxial processes of SiC, which were prepared from MTS- H_2 gaseous system, were performed in this work by using the finite element method. The chemistry kinetic model of gas-phase reactions employed in this work was proposed by other researchers. The total gas flow rate, temperature, and ratio of MTS/ H_2 were the main process parameters in this work, and their effects on consumption rate of MTS, molar fraction of intermediate species and C/Si ratio inside the hot reaction chamber were analyzed in detail. The phenomena of our simulations are interesting. Both low total gas flow rate and high substrate temperature have obvious effectiveness on increasing the consumption rate of MTS. For all cases, the highest three C contained intermediates are CH_4 , C_2H_4 and C_2H_2 , respectively, while the highest three Si/Cl contained intermediates are SiCl_2 , SiCl_4 and HCl , respectively. Furthermore, low total gas flow results in a uniform C/Si ratio at different temperatures, and reducing the ratio of MTS/ H_2 is an interesting way to raise the C/Si ratio in the reactor.

Keywords: chemical vapor deposition; gas phase reaction; MTS/ H_2 ratio; numerical model



Citation: Song, B.; Gao, B.; Han, P.; Yu, Y.; Tang, X. Numerical Simulation of Gas Phase Reaction for Epitaxial Chemical Vapor Deposition of Silicon Carbide by Methyltrichlorosilane in Horizontal Hot-Wall Reactor. *Materials* **2021**, *14*, 7532. <https://doi.org/10.3390/ma14247532>

Academic Editor: Giray Kartopu

Received: 5 November 2021

Accepted: 7 December 2021

Published: 8 December 2021

Publisher's Note: MDPI stays neutral with regard to jurisdictional claims in published maps and institutional affiliations.



Copyright: © 2021 by the authors. Licensee MDPI, Basel, Switzerland. This article is an open access article distributed under the terms and conditions of the Creative Commons Attribution (CC BY) license (<https://creativecommons.org/licenses/by/4.0/>).

1. Introduction

Since it has good performance on resistance to high temperature [1] and the ability to work under extremely harsh conditions with exceptional functionalities [2], silicon carbide (SiC) became an attractive material for power electronics and optoelectronics applications [1,3]. However, the deposition quality of SiC is still limited via chemical vapor deposition (CVD) processes [3], which constitute an important technology for the semi-conductor industry [4,5]. Horizontal [5–8] and vertical [9–12] reactors were widely used for CVD processes. High temperature CVD process in the hot-wall CVD reactor can achieve relatively high growth rates of SiC [13–15]. However, extreme high temperature conditions contributed undesirable increase of defects in the grown SiC films [16]. In this work the gas phase species were reacted in the temperature range of 900–1500 °C. Similar temperature distributions were employed in comparable investigations [12,16–18].

Different precursors [18–21] have been employed for the CVD processes of SiC. In comparison to the traditional CVD gas systems (such as SiH_4 - C_3H_8 - H_2 gaseous system), the addition of chloride contained species as precursors leads to an elevated deposition rate and optimized surface morphology [20]. The employment of chloride contained precursors is an elegant way to circumvent the problem with the silicon droplets in the CVD processes [22]. Methyltrichlorosilane (CH_3SiCl_3 , MTS) is one of the chlorides contained species and can be used as the precursor gas for hot-wall chemical vapor deposition of SiC [17,18,23]. MTS becomes an affordable precursor for CVD processes of SiC since it has good performance in

stoichiometric SiC deposition and can be facilitated at relatively lower temperature [12]. It decomposes in carrier gas to intermediate species, of which contribute greatly to deposition of the SiC film on the substrate surface [12,17].

Since researchers are interested in understanding and predicting the overall growth phenomena in CVD processes, calculations [7,12,17,18,20,24] of chemical kinetics coupling with heat and mass transfer and fluid dynamics were commonly used to investigate SiC growth process. Simulation models [12,17,18,23,25] with gas phase reactions of MTS-H₂ gaseous system were proposed by different researchers. However, thorough investigations focus on the effect of reactor temperature, MTS/H₂ ratio and total gas flow rate are still lacked. The desired composition of gas phase species inside the reactor greatly affected by the MTS/H₂ ratio, temperature and total flow rate [26]. Therefore, it is valuable to conduct thorough investigations on these conditions.

In the present work, the CVD model for the epitaxial growth process of SiC in a horizontal hot-wall reactor was simulated by using finite element method, which was widely employed in calculations for thermodynamic, computational fluid dynamics (CFD), and chemistry kinetic.

The carrier gas is hydrogen (H₂) and the precursor gas is MTS. Different conditions of temperature, MTS/H₂ ratio and total flow rate were employed in this work, and their effects on the consumption rate of precursor, molar fractions of major intermediates, and C/Si ratios based on important intermediates were analyzed in detail.

2. Simulation Modeling

Both chemical reaction kinetics and physical transfer phenomena are contained in these simulations. Additionally, assumptions proposed as [12,17,19]: (1) the mixture flow in the reactor is ideal laminar flow; (2) the gas-phase reactions are very fast; and (3) reaction expansion or contraction was neglected. Normally, physics applied in a CVD process which, using the dilute mixture approach, include three important parts: heat and mass transfer, fluid flow and chemistry [7]. The equations for mass and heat transfer are as follows [12] with time cumulative terms:

$$\rho C_p \frac{\partial T}{\partial t} + \nabla \cdot (-k \nabla T) + \rho C_p \vec{u} \cdot \nabla T = Q_r \quad (1)$$

$$\frac{\partial \rho}{\partial t} + \nabla \cdot \rho \vec{u} = 0 \quad (2)$$

$$\rho \frac{\partial \vec{u}}{\partial t} + \rho \vec{u} \cdot \nabla \vec{u} = -\nabla p + \nabla \cdot \left[\mu \nabla \vec{u} + (\nabla \vec{u})^T - \frac{2}{3} \mu \nabla \cdot \vec{u} \vec{I} \right] \quad (3)$$

$$\rho \frac{\partial w_i}{\partial t} + \nabla \cdot (-\rho D_i \nabla c w_i - D_i^T \nabla (\ln T)) + \rho (\vec{u} \cdot \nabla) w_i = M_i R_i \quad (4)$$

Here, Term \vec{I} is the identity tensor, T is temperature, R_i is reaction rate, M_i is molecular weight, Q_r is the external heat sources including radiation, C_p is heat capacity, and k is thermal conductivity, and D_i and D_i^T are the gas diffusion coefficient and the thermal diffusion coefficient, respectively. Subscript i denotes the i th gas species. The term \vec{u} is the vector of mass velocity, p is the pressure, ρ is the mixture mass density and here it is assumed as [1] $\rho = \frac{pM}{RT}$, where, R is the ideal gas constant, and M is the molar mass of the mixture gas [19].

The gas diffusivity at various temperatures and pressures was obtained using the kinetic theory of gases, and details can be found in references [26–29]. The properties of flow and heat transfer in the gas phase proposed by other researchers [7] were employed in this work.

Suppose there are i reactants and j products for each reversible reaction, then the reaction rate R_k for a reversible reaction can be given by [4]:

$$R_k = k_f \Pi \left(\frac{P f_i}{RT} \right)^{v_{if}} - k_b \Pi \left(\frac{P f_j}{RT} \right)^{v_{jb}} \quad (5)$$

where f_i (f_j) is mole fraction for the i th (j th) reactants (products) in the reaction, the k_f and k_b are forward reaction rate constant and reverse reaction rate constant, respectively, and v_{if} and v_{jb} are the forward and reverse stoichiometric coefficient, respectively. The reaction rate for each reaction follows the Arrhenius law [19]

$$k_{f,b} = AT^\beta \exp\left(\frac{-E}{RT}\right) \quad (6)$$

The value of A , β and E can be found in references [12,17]. The reverse reaction rate constant without terms A , β and E can be calculated by [4]:

$$k_b = \frac{k_f}{k_{eq}} \left(\frac{RT}{P^0} \right)^{(\sum_j v_{jb} - \sum_i v_{if})} \quad (7)$$

$$k_{eq} = \exp\left(-\frac{\Delta H - T\Delta S}{RT}\right) \quad (8)$$

where ΔH and ΔS are reaction enthalpy and reaction entropy, respectively. More details of the calculation method of these terms in Equations (5)–(8) can be found in references [4,19].

The simulations are performed in a simplified 2D model of a horizontal hot-wall CVD reactor (28 mm in internal diameter and the susceptor length is 100 mm). The distance from the inlet of quartz tube to susceptor is approximately 450 mm. Only the gas phase region is regarded as a numerical domain in this work [21,30]. The schematic of the computational gas phase domain above the susceptor is illustrated in Figure 1. There are 3 substrates (10 mm × 10 mm) located on the susceptor. The location of substrate 1 is close to flow inlet along the susceptor, while the location of substrate 3 is close to flow outlet along the susceptor. Horizontal line A is about 2 mm distance above the susceptor, and the vertical line B is from the center of substrate 2 to the upper wall. The line A and line B in succedent context imply the line A and line B indicated in Figure 1.

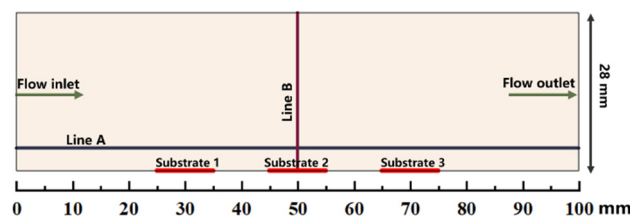


Figure 1. Schematic illustration of the computational gas phase domain above the susceptor.

Boundary conditions employed in the simulation model could keep as fixed values [18]. According to the research conditions, a constant temperature of reactor wall was fixed as 900 °C, and temperatures of substrate surfaces were fixed in constant values as listed in Table 1, in which includes the main research conditions in this work. The ratio of MTS/H₂ at the inlet of quartz tube is 25% for case 1, case 2, case 3 and case 4, and the total gas flow rate is lower for case 1 and case 2 while higher for case 3 and case 4. The ratio of MTS/H₂ at the inlet of quartz tube is 1.5% for case 5 and case 6. It should be noted that the inlet gas flow rate and the ratio of MTS/H₂ mentioned in succedent context indicate the gas flow rate and ratio at the inlet of quartz tube. Please note that we focus on the gas phase reactions mechanism in our simulations, the temperature conditions employed in this work are appropriate despite the temperature difference employed in this work either

between different substrates or between the substrates and the upper wall may seem exaggerated when compared with experimental situations.

Table 1. Calculation conditions in this work.

| | Substrate 1 Temp (°C) | Substrate 2 Temp (°C) | Substrate 3 Temp (°C) | H ₂ Flow (sccm) | MTS Flow (sccm) | Pressure (kPa) |
|--------|--------------------------|--------------------------|--------------------------|-------------------------------|--------------------|-------------------|
| Case 1 | 1000 | 1300 | 1100 | 100 | 25 | 6 |
| Case 2 | 1200 | 1500 | 1100 | 100 | 25 | 6 |
| Case 3 | 1000 | 1300 | 1100 | 5000 | 1250 | 20 |
| Case 4 | 1200 | 1500 | 1100 | 5000 | 1250 | 20 |
| Case 5 | 1000 | 1300 | 1100 | 5000 | 75 | 20 |
| Case 6 | 1200 | 1500 | 1100 | 5000 | 75 | 20 |

In order to facilitate the generation of regular meshes to improve the convergence of calculation, it is assumed that the substrate is adhered to the susceptor and the effect of geometry is neglected in this model. Since in the present work we focus on the gas phase reactions in the region above the susceptor, these assumptions can be considered reasonable.

The calculation results of gas phase reactions in the research of Kang Guan et al. [12] shows a good agreement with experiments, so it is reasonable to employ these gas phase reactions listed in their work in our simulations. Details of gas phase reaction equations and chemistry kinetics can be found in references [12,17] and not be repeated here. We focus on the gas phase reactions in this work and the effect of surface reaction mechanism is neglected.

3. Results and Discussion

As mentioned in Section 2, since we focus on the gas phase reactions in the reactor, the main growth conditions were kept as fixed values in our calculations. Chemistry kinetics, computational fluid dynamics, and heat and mass transfer coupled in the models deliver great contributions in these simulations to calculate the temperature distribution, gas phase velocity distribution, and molar fractions of intermediate species formed inside the reactor for each case. Some of the gas phase intermediates play important role in surface reactions, the C/Si ratio based on these species will also be discussed.

Velocity of the gas phase above the susceptor is shown in Figure 2 with same scale, the X direction is the flow direction, and the color bar for all subfigures is illustrated in the right end. It should be noted that the velocity distribution employed in this work was calculated under the standard conditions based on the total gas flow rate at the inlet of the quartz tube. It is obviously that when the ratio of MTS/H₂ is fixed at 25% the flow velocity is highest in case 3 and case 4 and lowest in case 1 and case 2 cause the former have the higher carrier gas flow rate. The flow velocity plays an important role in precursor consumption rate and this will be discussed in the following context.

The molar fractions of MTS in different cases from substrate to the upper wall along line B are illustrated in Figure 3a. Additionally, the MTS consumption rate defined as the ratio of consumed MTS to the initial MTS fraction is illustrated along line B in Figure 3b. When the MTS/H₂ ratio is fixed at 25%, the MTS molar fraction increases with the decrease of substrate temperature or increase of total flow rate, since the lower temperature or higher gas flow velocity will reduce MTS consumption rate. When the carrier gas flow rate is fixed at 5000 sccm, reduce the MTS/H₂ ratio led to more consumption of MTS.

Normally in CVD process, the deposition on substrate surface is usually contributed by intermediates of gas phase reactions instead of precursors [23,25]. It seems when the substrate temperature is high and the total gas flow rate is low, the consumption rate of MTS will increase greatly. Therefore, most of MTS gas will decompose into intermediate species. Decreasing the substrate temperature or increasing either the gas flow rate or the ratio of MTS/H₂ will reduce the consumption rate of MTS. In the situation that the total gas flow rate is very low (case 1 and case 2), the consumption rate of MTS is close to 1.

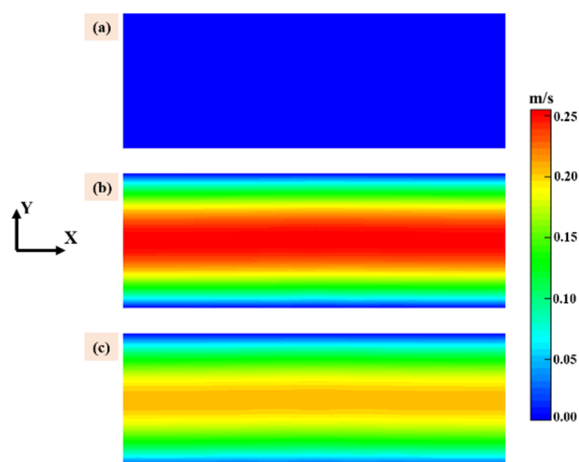


Figure 2. Velocity of the gas phase above the susceptor: (a) case 1 and case 2; (b) case 3 and case 4; and (c) case 5 and case 6.

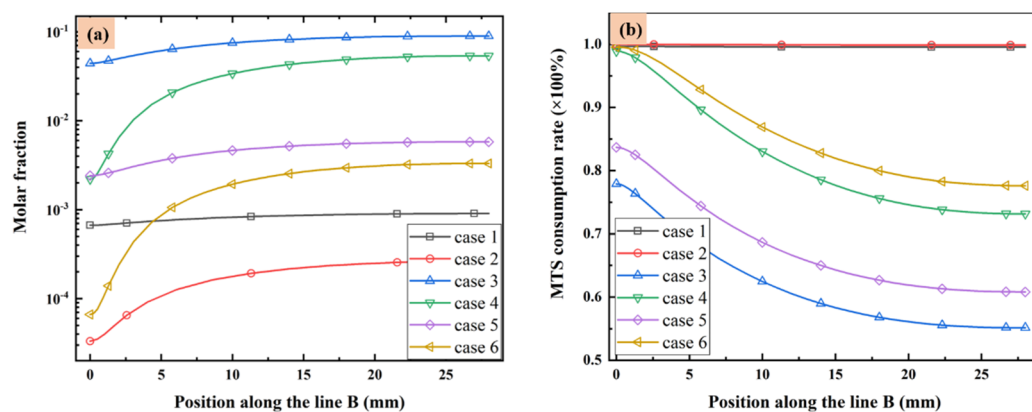


Figure 3. (a) MTS molar fraction and (b) MTS consumption rate along line B.

MTS decomposes quickly in the reactor and intermediates are produced. Since we are interested in the compositions of gas phase species close to the substrate surface, the molar fractions of main intermediate species formed above the susceptor are discussed in detail, along line A (as indicated in Figure 1) from gas inlet to outlet. Figures 4 and 5 show the predicted molar fractions of important C contained species and Si/Cl contained species at different cases, respectively. The molar fractions which greater than 10^{-7} are taken along line A from the flow inlet direction. The most three C contained intermediates (major C contained intermediates) are CH_4 , C_2H_4 and C_2H_2 , respectively, while the most three Si/Cl contained intermediates (major Si/Cl contained intermediates) are SiCl_2 , SiCl_4 and HCl , respectively. It seems that the ratio of MTS/H_2 and total gas flow rate have significant effect on the fractions for intermediate compositions. The molar fractions of major C contained intermediates are relatively lower than major Si/Cl contained intermediates. The increase of temperature will promote the composing of some intermediate species like C_2H_2 , SiCl_2 , etc., so the formation of other intermediate species like C_2H_3 , SiH_3Cl , etc., will be inhibited.

Besides, when the ratio of MTS/H_2 is 25%, the molar fractions of major C contained intermediates and major Si/Cl contained intermediates decrease with increase of total flow rate. It is caused by the decrease of MTS consumption rate shown in Figure 3. When the ratio of MTS/H_2 is 25% at lower gas flow rate, the most abundant C contained intermediate is CH_4 at lower temperature and changes to C_2H_2 with increasing temperature. Furthermore, CH_4 is the most abundant C contained intermediate for all cases when the carrier gas flow rate is 5000 sccm.

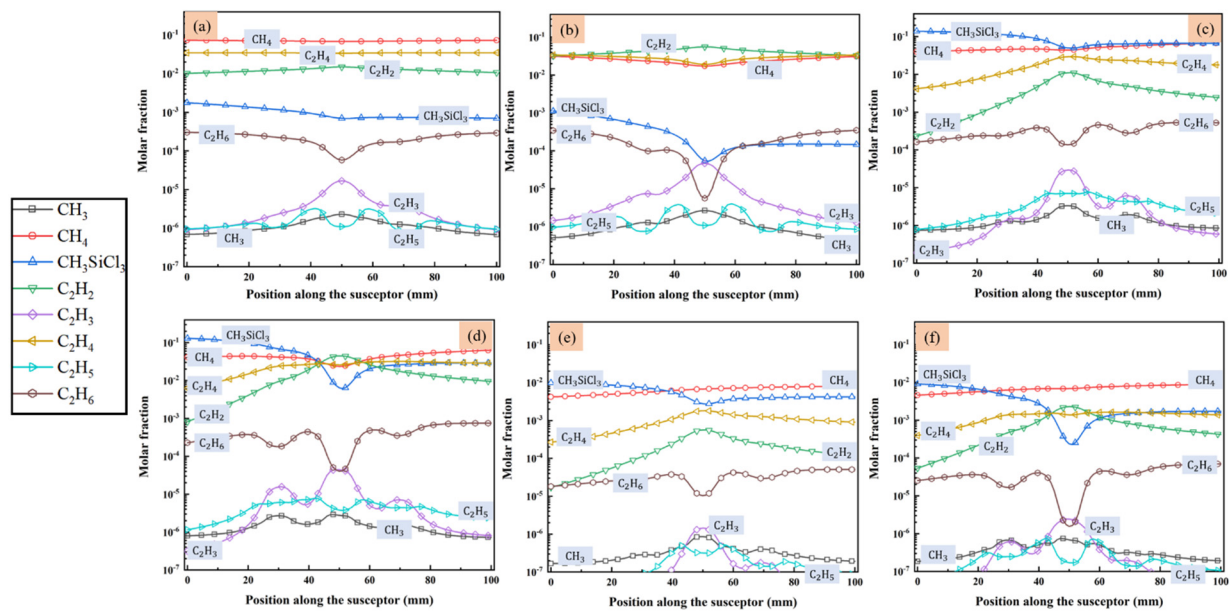


Figure 4. The molar fraction of main species that contained C in the gas phase above the susceptor: (a) case 1; (b) case 2; (c) case 3; (d) case 4; (e) case 5; and (f) case 6.

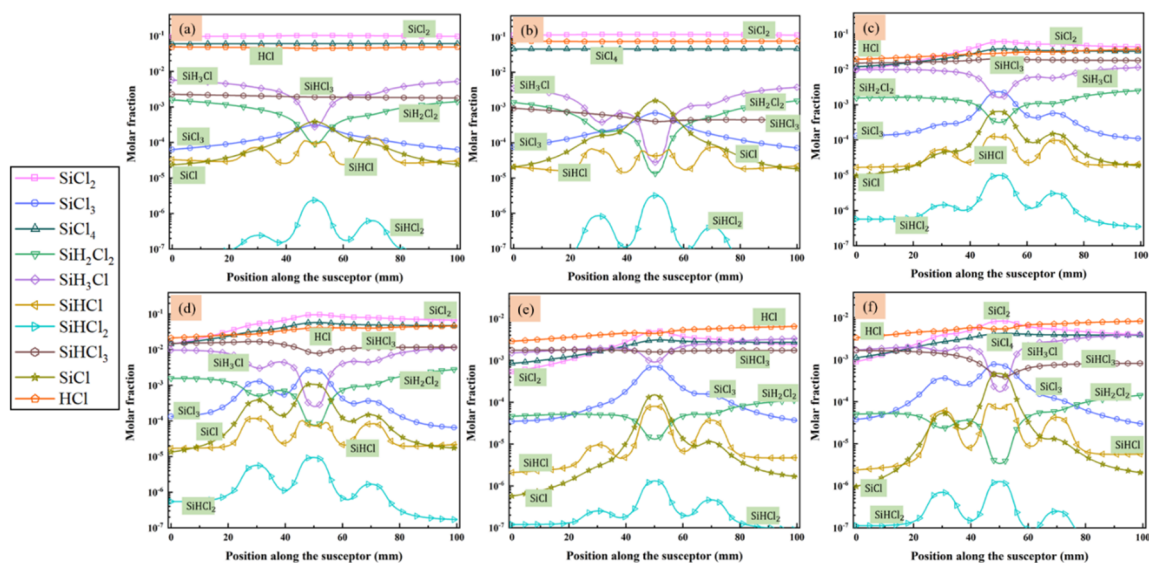


Figure 5. The molar fraction of main species that contained Si/Cl in the gas phase above the susceptor: (a) case 1; (b) case 2; (c) case 3; (d) case 4; (e) case 5; and (f) case 6.

When the ratio of MTS/H₂ is 25%, the most abundant Si/Cl contained intermediate is SiCl₂. SiCl₂ allows higher deposition temperatures and restrains the formation of silicon clusters on the film surface and has high surface activity [20]. Therefore, there is high possibility of chemically stability in cases 1–4. HCl becomes the most abundant Si/Cl contained intermediate when the ratio of MTS/H₂ decrease to 1.5%. Researchers [12,31,32] pointed out that HCl highly affects the growth rate and is involved in the deposition because of its etching effect on SiC film. It implies that HCl has a greater effect on the growth rate at low MTS/H₂ ratio in case 5 and case 6 than at high MTS/H₂ ratio in case 3 and case 4.

Researchers [12,17] have proposed a series of modified surface reactions based on the MTS-H₂ gaseous system. Surface reactions in which C or Si contained intermediate species participate as reactants are listed in Table 2, including atom adsorption reactions, and reactions between gaseous and surface species.

Table 2. List of surface reactions in which C or Si contained intermediate species participate as reactants from references [12,17].

| Reaction on Bulk Silicon Carbide Surface * | |
|----------------------------------------------------------------------------------------------------------------------------------------------------------------------------|--------------------------------------------------------------------------------------------------------------------------------------------------------|
| $\text{SiHCl}_3 + 2\text{Si}(\$) + 2\text{C}(\$) \rightarrow \text{SiCl}(\text{S}) + \text{H}(\text{S}) + 2\text{Cl}_{\text{Si}}(\text{S})$ | $\text{SiCl}_4 + 2\text{Si}(\$) + 2\text{C}(\$) \rightarrow \text{SiCl}(\text{S}) + \text{Cl}_{\text{C}}(\text{S}) + 2\text{Cl}_{\text{Si}}(\text{S})$ |
| $\text{SiHCl}_3 + \text{Si}(\$) + 3\text{C}(\$) \rightarrow \text{SiCl}(\text{S}) + \text{H}(\text{S}) + \text{Cl}_{\text{C}}(\text{S}) + \text{Cl}_{\text{Si}}(\text{S})$ | $\text{SiH}_2\text{Cl}_2 + \text{Si}(\$) + 3\text{C}(\$) \rightarrow \text{SiCl}(\text{S}) + 2\text{H}(\text{S}) + \text{Cl}_{\text{Si}}(\text{S})$ |
| $\text{SiH}_3\text{Cl} + 2\text{C}(\$) \rightarrow \text{SiCl}(\text{S}) + \text{H}(\text{S}) + \text{H}_2$ | $\text{C}_2\text{H}_6 + 2\text{Si}(\$) \rightarrow 2\text{C}(\text{S}) + 3\text{H}_2$ |
| $\text{C}_2\text{H}_4 + 2\text{Si}(\$) \rightarrow 2\text{C}(\text{S}) + 2\text{H}_2$ | $\text{C}_2\text{H}_3 + 2\text{Si}(\$) \rightarrow \text{C}(\text{S}) + \text{CH}(\text{S}) + \text{H}_2$ |
| $\text{C}_2\text{H}_2 + 2\text{Si}(\$) \rightarrow 2\text{C}(\text{S}) + \text{H}_2$ | $\text{CH}_4 + \text{Si}(\$) \rightarrow \text{C}(\text{S}) + 2\text{H}_2$ |
| $\text{SiCl}_3 + 2\text{C}(\$) + \text{Si}(\$) \rightarrow \text{SiCl}(\text{S}) + \text{Cl}_{\text{C}}(\text{S}) + \text{Cl}_{\text{Si}}(\text{S})$ | $\text{SiCl}_3 + \text{C}(\$) + 2\text{Si}(\$) \rightarrow \text{SiCl}(\text{S}) + 2\text{Cl}_{\text{Si}}(\text{S})$ |
| $\text{SiCl}_3 + 3\text{C}(\$) \rightarrow \text{SiCl}(\text{S}) + 2\text{Cl}_{\text{C}}(\text{S})$ | $\text{SiHCl} + \text{C}(\$) \rightarrow \text{Si}(\text{S}) + \text{HCl}$ |
| $\text{SiCl} + \text{C}(\$) \rightarrow \text{SiCl}(\text{S})$ | $2\text{Cl}_{\text{C}}(\text{S}) + \text{SiCl}_2 \rightarrow \text{SiCl}_4 + 2\text{C}(\$)$ |
| $\text{SiCl}_2 + 2\text{C}(\$) \rightarrow \text{SiCl}(\text{S}) + \text{Cl}_{\text{C}}(\text{S})$ | $\text{Cl}_{\text{Si}}(\text{S}) + \text{Cl}_{\text{C}}(\text{S}) + \text{SiCl}_2 \rightarrow \text{SiCl}_4 + \text{Si}(\$) + \text{C}(\$)$ |
| $\text{SiCl}_2 + \text{Si}(\$) + \text{C}(\$) \rightarrow \text{SiCl}(\text{S}) + \text{Cl}_{\text{Si}}(\text{S})$ | |

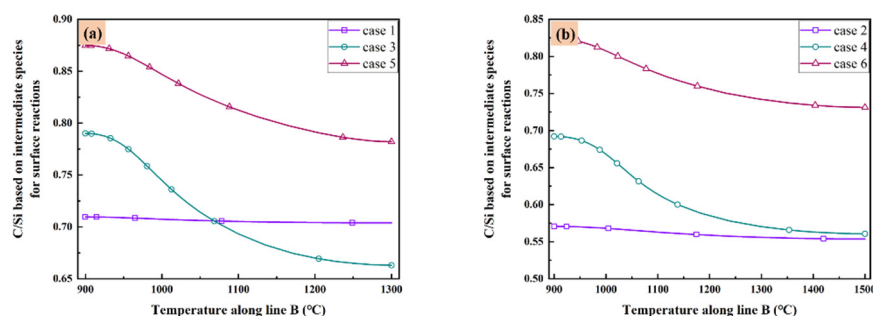
* In this table, S designates surface species, and Si(\$\$) and C(\$\$) represent Si and C surface sites, respectively. Subscripts C and Si indicate a molecule absorbed on C or Si sites.

It can be seen, C contained gas phase intermediates consume empty sites on Si surfaces then produce surface species with C sites (C(S) and CH(S)). Additionally, Si contained gas phase intermediates consume empty sites on both C and Si surfaces then produce surface species with Si sites (SiCl(S), Si(S), H(S) and Cl_C(S)) and C sites (Cl_{Si}(S)). Therefore, these gas phase intermediates listed in Table 3 participate as reactants in surface reactions contribute directly to produce surface species.

Table 3. List of C or Si contained intermediate species participate as reactants.

| C Contained Species | Si Contained Species |
|-------------------------------------------------------------------------------------------------------------------------------------------------|------------------------------------------------------------------------------------------------------------------------------------------------------|
| C ₂ H ₆ , C ₂ H ₄ , C ₂ H ₃ , C ₂ H ₃ , CH ₄ | SiH ₃ Cl, SiHCl ₃ , SiH ₂ Cl ₂ , SiCl ₄ , SiCl ₃ , SiCl ₂ , SiCl, SiHCl |

As listed in Table 3, there are five C contained species and eight Si contained species play important role in the surface reaction model. These species are the most important intermediate species contributing to the surface reactions in gas phase. Therefore, it is valuable to discuss the distribution of C/Si ratios based on all above species in the reactor of all cases. The C/Si ratios for all cases based on all the intermediate species in Table 3 are illustrated in Figure 6 as the function of temperature along line B. It seems the low temperature corresponding to the high C/Si ratio in all cases. When the total gas flow rate is low enough as in case 1 and case 2, the difference of C/Si ratio is very small at different temperature. Additionally, when the total gas flow rate is fixed, higher substrate temperature means lower C/Si ratio. However, if you have a preference of higher C/Si ratio, increasing the total gas flow rate may satisfy your purpose when the substrate temperature is high as 1500 °C. Furthermore, decrease the MTS/H₂ ratio within a reasonable range seems a more elegance way since both case 5 and case 6 have higher C/Si ratio at different substrate temperatures.

**Figure 6.** C/Si ratio based on intermediate species for surface reactions as the function of temperature along line B: (a) case 1, case 3 and case 5; and (b) case 2, case 4 and case 6.

4. Conclusions

Simulations of the MTS-H₂ gaseous system occurring in a two-dimensional horizontal hot-wall CVD reactor model were calculated by using finite element method. The gas phase reaction equations and kinetics were obtained from the literature, and surface reaction kinetics were not considered. The temperature range of substrates was 1000–1500 °C, the range of carrier gas flow rates was 100–5000 sccm, and the ratio of MTS/H₂ was fixed at 25% or 1.5%.

The results of simulations indicated that both the temperature and total flow rate show a distinct effect on consumption rate of MTS. For all cases, CH₄, C₂H₄, C₂H₂, SiCl₂ and SiCl₄ are the abundant C or Si contained intermediate species in the reactor. Increasing temperature will promote the composing of some intermediates like C₂H₂ and SiCl₂, so the formation of other intermediates like C₂H₃ and SiH₃Cl will be inhibited. HCl which was proved highly affecting the growth rate in other literatures becomes to be the most abundant Si/Cl contained intermediate when the ratio of MTS/H₂ is 1.5%. The C/Si ratio based on intermediates which participate as reactants in surface reactions in the reactor, becomes uniform at different temperatures when the total gas flow rate is low, and increases when reducing the ratio of MTS/H₂.

Author Contributions: Conceptualization, B.S. and B.G.; Data curation, B.S.; Software, B.S.; Supervision, B.G.; Validation, P.H. and X.T.; Visualization, Y.Y.; Writing—original draft, B.S.; Writing—review & editing, B.S. and B.G.; funding acquisition, B.G. All authors have read and agreed to the published version of the manuscript.

Funding: This research received no external funding.

Institutional Review Board Statement: Not applicable.

Informed Consent Statement: Not applicable.

Data Availability Statement: Not applicable.

Conflicts of Interest: The authors declare no conflict of interest.

References

1. Allendorf, M.D.; Kee, R.J. A model of silicon-carbide chemical vapor-deposition. *J. Electrochem. Soc.* **1991**, *138*, 841–852. [[CrossRef](#)]
2. Powell, J.A.; Will, H.A. Epitaxial growth of 6H SiC in the temperature range 1320–1390 °C. *J. Appl. Phys.* **1973**, *44*, 5177–5178. [[CrossRef](#)]
3. Fiorucci, A.; Moscatelli, D.; Masi, M. Homoepitaxial silicon carbide deposition processes via chlorine routes. *Surf. Coat. Technol.* **2007**, *201*, 8825–8829. [[CrossRef](#)]
4. Kleijn, C.R. Computational modeling of transport phenomena and detailed chemistry in chemical vapor deposition—A benchmark solution. *Thin Solid Film.* **2000**, *365*, 294–306. [[CrossRef](#)]
5. Danielsson, O.; Henry, A.; Janzen, E. Growth rate predictions of chemical vapor deposited silicon carbide epitaxial layers. *J. Cryst. Growth.* **2002**, *243*, 170–184. [[CrossRef](#)]
6. Ji, W.; Lofgren, P.M.; Hallin, C.; Gu, C.Y.; Zhou, G. Computational modeling of SiC epitaxial growth in a hot wall reactor. *J. Cryst. Growth* **2000**, *220*, 560–571. [[CrossRef](#)]
7. Lofgren, P.M.; Ji, W.; Hallin, C.; Gu, C.Y. Modeling of silicon carbide epitaxial growth in hot-wall chemical vapor deposition processes. *J. Electrochem. Soc.* **2000**, *147*, 164–175. [[CrossRef](#)]
8. Danielsson, O.; Forsberg, U.; Henry, A.; Janzen, E. Investigation of the temperature profile in a hot-wall SiC chemical vapor deposition reactor. *J. Cryst. Growth* **2002**, *235*, 352–364. [[CrossRef](#)]
9. Vorob'ev, A.N.; Egorov, Y.E.; Makarov, Y.N.; Zhmakin, A.I.; Galyukov, A.O.; Rupp, R. Modeling of silicon carbide chemical vapor deposition in a vertical reactor. *Mat. Sci. Eng. B* **1999**, *61–62*, 172–175. [[CrossRef](#)]
10. Rupp, R.; Makarov, Y.N.; Behner, H.; Wiedenhofer, A. Silicon carbide epitaxy in a vertical CVD reactor: Experimental results and numerical process simulation. *Phys. Status Solidi B* **1997**, *202*, 281–304. [[CrossRef](#)]
11. Vorob'ev, A.N.; Karpov, S.Y.; Bogdanov, M.V.; Komissarov, A.E.; Bord, O.V.; Zhmakin, A.I.; Makarov, Y.N. Numerical study of SiCCVD in a vertical cold-wall reactor. *Comp. Mater. Sci.* **2002**, *24*, 520–534. [[CrossRef](#)]
12. Guan, K.; Gao, Y.; Zeng, Q.F.; Luan, X.G.; Zhang, Y.; Cheng, L.F.; Wu, J.Q.; Lu, Z.Y. Numerical modeling of SiC by low-pressure chemical vapor deposition from methyltrichlorosilane. *Chin. J. Chem. Eng.* **2020**, *28*, 1733–1743. [[CrossRef](#)]
13. Masahara, K.; Takahashi, T.; Kushibe, M.; Ohno, T.; Nishio, J.; Kojima, K.; Ishida, Y.; Suzuki, T.; Tanaka, T.; Yoshida, S.; et al. High-rate epitaxial growth of 4H-SiC using a vertical-type, quasi-hot-wall CVD reactor. *Mater. Sci. Forum* **2002**, *389–393*, 179–182. [[CrossRef](#)]

14. Kordina, O.; Hallin, C.; Henry, A.; Bergman, J.P.; Ivanov, I.; Ellison, A.; Son, N.T.; Janzen, E. Growth of SiC by “hot-wall” CVD and HTCVD. *Phys. Status Solidi B* **1997**, *202*, 321–334. [[CrossRef](#)]
15. Ellison, A.; Zhang, J.; Magnusson, W.; Henry, A.; Wahab, Q.; Bergman, J.P.; Hemmingsson, C.; Son, N.T.; Janzen, E. Fast SiC epitaxial growth in a chimney CVD reactor and HTCVD crystal growth developments. *Mater. Sci. Forum* **2000**, *338–342*, 131–136. [[CrossRef](#)]
16. Myers, R.L.; Shishkin, Y.; Kordina, O.; Sadow, S.E. High growth rates (>30 $\mu\text{m/h}$) of 4H-SiC epitaxial layers using a horizontal hot-wall CVD reactor. *J. Cryst. Growth* **2005**, *285*, 486–490. [[CrossRef](#)]
17. Guan, K.; Zeng, Q.; Liu, Y.; Luan, X.; Lu, Z.; Wu, J. A multiscale model for CVD growth of silicon carbide. *Comp. Mater. Sci.* **2021**, *196*, 110512. [[CrossRef](#)]
18. Leone, S.; Kordina, O.; Henry, A.; Nishizawa, S.; Danielsson, O.; Janzen, E. Gas-phase modeling of chlorine-based chemical vapor deposition of silicon carbide. *Cryst. Growth Des.* **2012**, *12*, 1977–1984. [[CrossRef](#)]
19. Meziere, J.; Ucar, M.; Blanquet, E.; Pons, M.; Ferret, P.; Di Cioccio, L. Modeling and simulation of SiC CVD in the horizontal hot-wall reactor concept. *J. Cryst. Growth* **2004**, *267*, 436–451. [[CrossRef](#)]
20. Wang, R.; Ma, R.H.; Dudley, M. Reduction of chemical reaction mechanism for halide-assisted silicon carbide epitaxial film deposition. *Ind. Eng. Chem. Res.* **2009**, *48*, 3860–3866. [[CrossRef](#)]
21. Nishizawa, S.; Pons, M. Growth and doping modeling of SiC-CVD in a horizontal hot-wall reactor. *Chem. Vap. Depos.* **2006**, *12*, 516–522. [[CrossRef](#)]
22. Pedersen, H.; Leone, S.; Kordina, O.; Henry, A.; Nishizawa, S.; Koshka, Y.; Janzen, E. Chloride-based cvd growth of silicon carbide for electronic applications. *Chem. Rev.* **2012**, *112*, 2434–2453. [[CrossRef](#)] [[PubMed](#)]
23. Lu, C.Y.; Cheng, L.F.; Zhao, C.N.; Zhang, L.T.; Xu, Y.D. Kinetics of chemical vapor deposition of SiC from methyltrichlorosilane and hydrogen. *Appl. Surf. Sci.* **2009**, *255*, 7495–7499. [[CrossRef](#)]
24. Cavallotti, C.; Rossi, F.; Ravasio, S.; Masi, M. A Kinetic analysis of the growth and doping kinetics of the SiC chemical vapor deposition process. *Ind. Eng. Chem. Res.* **2014**, *53*, 9076–9087. [[CrossRef](#)]
25. Fukushima, Y.; Sato, N.; Funato, Y.; Sugiura, H.; Hotozuka, K.; Momose, T.; Shimogaki, Y. Multi-scale analysis and elementary reaction simulation of SiC-CVD using $\text{CH}_3\text{SiCl}_3/\text{H}_2$. *ECS J. Solid State Sci. Technol.* **2013**, *2*, P492. [[CrossRef](#)]
26. Deivendran, B.; Shinde, V.M.; Kumar, H.; Prasad, N.E. 3D Modeling and optimization of SiC deposition from $\text{CH}_3\text{SiCl}_3/\text{H}_2$ in a commercial hot wall reactor. *J. Cryst. Growth* **2021**, *554*, 125944. [[CrossRef](#)]
27. Mousavipour, S.H.; Saheb, V.; Ramezani, S. Kinetics and mechanism of pyrolysis of methyltrichlorosilane. *J. Phys. Chem. A* **2004**, *108*, 1946–1952. [[CrossRef](#)]
28. Brokaw, R.S. Predicting transport properties of dilute gases. *Ind. Eng. Chem. Process. Des. Dev.* **1969**, *8*, 240–253. [[CrossRef](#)]
29. Neufeld, P.D.; Janzen, A.R.; Aziz, R.A. Empirical equations to calculate 16 of the transport collision integrals $\Omega(l, s)^*$ for the Lennard-Jones (12–6) potential. *J. Chem. Phys.* **1972**, *57*, 1100–1102. [[CrossRef](#)]
30. Nishizawa, S.; Pons, M. Numerical modeling of SiC-CVD in a horizontal hot-wall reactor. *Microelectron Eng.* **2006**, *83*, 100–103. [[CrossRef](#)]
31. Wang, R.; Ma, R.H. An integrated model for halide chemical vapor deposition of silicon carbide epitaxial films. *J. Cryst. Growth* **2008**, *310*, 4248–4255. [[CrossRef](#)]
32. Wang, R.; Ma, R.H. Kinetics of halide chemical vapor deposition of silicon carbide film. *J. Cryst. Growth* **2007**, *308*, 189–197. [[CrossRef](#)]